

We are IntechOpen, the world's leading publisher of Open Access books Built by scientists, for scientists

6,900

Open access books available

186,000

International authors and editors

200M

Downloads

Our authors are among the

154

Countries delivered to

TOP 1%

most cited scientists

12.2%

Contributors from top 500 universities



WEB OF SCIENCE™

Selection of our books indexed in the Book Citation Index
in Web of Science™ Core Collection (BKCI)

Interested in publishing with us?
Contact book.department@intechopen.com

Numbers displayed above are based on latest data collected.
For more information visit www.intechopen.com



Active Flow Control of Wind Turbine Blades

Victor Maldonado

Additional information is available at the end of the chapter

<http://dx.doi.org/10.5772/63480>

Abstract

Active flow control is a technique to improve the fluid dynamics of an aerodynamic body utilizing an active actuator and energy input. Much progress on the application of active flow control techniques for wind turbine blades has been accomplished in the last decade. The main focus has been on regulating unsteady aerodynamic blade loads and vibration by controlling the flow locally along the blade. The trailing edge flap and synthetic jet actuator have emerged among the most effective actuators for wind turbines. This chapter gives an overview of active flow control techniques, with a specific focus on the application and use of the piezoelectric synthetic jet for vibration reduction of small-scale wind turbine blade models tested in a wind tunnel. Using the techniques presented, the global flow field over the blade was altered such that flow separation was mitigated. Consequently, this resulted in a significant decrease in the vibration of the blade. Particle image velocimetry (PIV) was used to quantify the flow field over the blade. Using synthetic jets, the flow over the blade was either fully or partially reattached, depending on the angle of attack. Current and future research in this field has evolved to understanding and controlling realistic 3D vortex flows typical of actual wind turbines utilizing scaled-down rotor platforms. To this end, the author presents the design and operation of a rotor test tower with custom blades embedded with synthetic jet actuators aimed at investigating multi-scale blade tip vortex interaction and breakdown that may lead to blade vibration and noise reduction.

Keywords: active flow control, wind turbines, synthetic jets, load, vibration control

1. Introduction

As the desire to harvest more energy from the wind by increasing the rotor diameter of modern wind turbines continues, wind turbine manufacturers seek to implement techniques that reduce blade load fluctuations and structural vibration. The use of variable-speed and individual blade

pitch control rotors (used in most modern large-scale turbines) offers an efficiency increase by allowing the turbine to operate closer to its maximum aerodynamic performance at a wider range of wind speeds, thus extracting more energy from the wind.

Active flow control is a method to selectively manipulate the flow field around certain portions of the blade in response to the local wind conditions in order to bring about a desirable effect. Active flow control requires external energy or auxiliary power; therefore, the benefit of the technique (e.g., in terms of increase in power output or blade lifetime) must offset the external energy or additional capital/maintenance costs required for flow control. There are various examples of active flow control devices, for example; trailing edge flaps or microtabs for laboratory scale non-rotating wind turbine blades [1–4] and large-scale industry wind turbines [5–11], or trailing edge synthetic jets for circulation control [12], air-jet vortex generators on the surface of the blade [13], and plasma actuators to control aerodynamic loading and separation [14, 15]. Two of the most common types of actuators are the piezoelectric synthetic jet and the dielectric barrier discharge or plasma actuator. The former utilizes a piezoelectric disk as a diaphragm to ingest and expel air surrounding a cavity at high frequency, and the latter ionizes the air surrounding two electrodes such that the air is accelerated through an electric field. In the active flow control methods that follow, we focus our discussion on piezoelectric-based synthetic jet actuators.

Much of the work on synthetic jet actuators has focused largely on control of separation on fixed-pitch (non-rotating) blades. Separation control is achieved by exploiting the narrow-band receptivity of the separating shear layer and the upstream boundary layer to external actuation [16]. Oster and Wygnanski [17] and Roberts [18] showed that the actuation can affect the global flow field by modifying the evolution and interactions of the large-scale vortical structures. These modifications can lead to a Coanda-like deflection of the separating shear layer toward the surface [19] such that the layer vortices are advected downstream in close proximity to the surface. This approach has been implemented, with varying degrees of success and different actuation means, to restore aerodynamic performance of stalled airfoils and flaps [20–21]. In particular, Seifert et al. [19] and Wygnanski [22] argued that the actuation is most effective when its period scales with the advection time over the length of the flow domain downstream of separation as measured by the reduced frequency F^+ . Therefore, when the separation domain scales with the characteristic length of an aerodynamic body, the (dimensionless) actuation frequency can couple to, and even drive the shedding frequency in the near wake. The possibility of coupling between (nominally) time-periodic shedding of coherent vortices and the separated shear layer in the absence of actuation is intriguing because such feedback between the near-wake instabilities and the separating shear layer is even more pronounced in the presence of actuation, thereby amplifying the unsteady component of the global aerodynamic forces. The approach of coupling the actuation frequency to instabilities relies explicitly on the narrow-band receptivity of the separating shear layer to a control input that is effective within a limited spatial domain immediately upstream of separation. Furthermore, when the flow is not separated, the effectiveness of this approach diminishes.

Another approach to control the flow is based on fluidic modification of the apparent aerodynamic shape of lifting surfaces using integrated synthetic jets that are driven at high

frequencies (i.e., much larger than the characteristic frequencies of the flow); this approach was presented by Amitay and Glezer [23]. Thus, it does not necessarily rely on coupling to global flow instability and therefore can be applied over a broader range of flow conditions [24, 25]. Furthermore, this approach can accommodate broader band control algorithms when more complex actuation waveforms are used such as the pulse modulation technique [26, 27]. The modification of aerodynamic characteristics of an unconventional airfoil with synthetic jets [27] has demonstrated that flow separation at high angles of attack can be mitigated or altogether suppressed by appropriate dynamic tailoring of the apparent surface curvature (and thus the distribution of the stream-wise pressure gradient) in advance of the onset of separation.

Some studies have attempted to take a classical feedback control approach to controlling the flow and its desired performance advantage. The modeling and closed-loop control of fluid flow is widely recognized as a challenging multidisciplinary effort [28] requiring expertise in fluid dynamics, sensor and actuator design, and modeling and control design. In the literature, three primary strategies exist for closed-loop control of fluid flow [29] (i) a model-independent approach based on empirical controller tuning, (ii) a full-order optimal control solution based on the solution of the Navier-Stokes equation, and (iii) approaches based on reduced-order models. To achieve reliable performance and robustness, the model-independent approach is not appropriate. For implementation in real time, a full-order solution is computationally impractical. Much current literature relates to the reduced-order approach to flow modeling. A variety of approaches have been taken to develop reduced-order models; these include the representation of the flow system by linear transfer functions [30] using system identification techniques to obtain experimental transfer function model [31, 32] and proper orthogonal decomposition (POD) [33] performed with experimental particle image velocimetry (PIV) data on a model wind turbine array [34] and most recently on a wind turbine blade in dynamic stall [35].

The goal of this chapter is to present to the reader some of the most common experimental active flow control techniques familiar to the author and new developments in the field. It is by no means an exhaustive or detailed review; rather it serves to acquaint the reader with the basic knowledge and significance of active flow control for wind turbine blades.

2. Experimental techniques

The experimental techniques utilized to conduct research in active flow control of wind turbines can be classified into three broad categories: (i) the wind turbine blade design and fabrication, (ii) the active flow control technique (e.g., synthetic jets or plasma actuators), and (iii) the equipment and facilities required to analyze the characteristics or behavior of the blade. We begin our treatment with a general description of the techniques utilized to design and fabricate turbine blades, and then focus our attention on rapid prototyping techniques with a specific example of wind turbine blade model fabricated from stereolithography and tested inside a wind tunnel. The instrumentation of these blades with piezoelectric-based synthetic

jet actuators and sensors is also discussed. Additional equipment to quantify some physical phenomena, typically the fluid dynamics of the blade to evaluate the effectiveness of the flow control is also required. This is normally accomplished by testing the wind turbine blade inside a wind tunnel where the upstream flow conditions are known and can be controlled. The most common experimental techniques including the use of wind tunnel facilities to test the performance of wind turbine blades are examined below.

2.1. Wind turbine blade design and fabrication

Modern wind turbine blades are created with a combination of computer design tools (e.g., computer-aided design (CAD) and computational fluid dynamics) and advanced composite materials and fabrication techniques [36]. The scale and application of the blade are very important in determining the exact materials and fabrication process. The majority of consumer- and utility-scale wind turbine blades utilized to generate electric power are manufactured from composite materials such as carbon fiber. Their high strength-to-weight ratio translates into an ability to withstand high load conditions with low rotational inertia. This key characteristic contributes to the manufacture of increasingly large wind turbine rotor diameters, which is a trend in the wind energy industry to reduce the cost of energy to compete with traditional fossil fuels.

Wind turbine blades that we can refer to as experimental and sometimes not utilized to generate electric power are often manufactured from a variety of rapid prototyping techniques and materials. The scale of these blades is relatively small, and custom-design requirements are needed. The main design considerations for blades utilizing active flow control include (i) modularity to assemble/disassemble the blade in multiple sections with a common core spar, (ii) accessibility and features to mount the actuators and sensors, and (iii) mounting mechanism of the blade. Design modularity is an important feature for experimental blade design that is considered in the conceptual design and solid CAD modeling stage. Utilizing active flow control and measuring the fluid dynamics of an original blade may prompt new insight into how changes in the design or geometry of the flow control actuator can improve the behavior or aerodynamics of the blade. As the blade is fabricated in modules, redesigning and rapid prototyping a new module with different design features is easier and more cost-effective than creating a new blade. Multiple blade modules also make it easier to access and manipulate the blade when applying actuators and sensors, which are placed in precise locations. For these reasons, the combination of CAD modeling and rapid prototyping are ideal tools to develop experimental wind turbine blades. Finally, we must consider how the blade will be mounted and design the proper mechanism or adapter. In most cases, the blade will be tested inside of a wind tunnel where the blade may be mounted to a load cell or pitching mechanism to change the pitch angle.

An example of an experimental wind turbine blade model developed by the author is shown in **Figure 1**. It contains an S809 airfoil profile, which is an airfoil developed by the National Renewable Energy Laboratory (NREL) for wind turbine operation [37]. The geometry of the blade includes a span of 0.457 m and a taper ratio of 0.688 (the tip chord divided by the root chord) where the root chord is 0.203 m. The model was designed in the Unigraphics CAD

package and is modular; it contains four modules with three additional removable surfaces to access the piezoelectric disk actuators. The modules and surfaces screw into a common aluminum spar. The model is rapid prototyped with a stereolithography technique with a material tensile strength of about 65 MPa. The blade contains a total of 14 synthetic jet-based piezo-actuators: 4 closest to the root and 5 in the middle and tip portions of the blade as shown. The synthetic jet orifices have a width of 0.75 mm and a length of 10 mm and are located at chord-wise location of x/c of 0.318 parallel to the blade leading edge. Each synthetic jet is individually controlled and driven with a 20-mm piezo disk. The optimum piezo-actuation frequency of 2100 Hz was determined from calibration discussed in the next section. Finally, the blade contains two strain gauges (in a Wheatstone bridge arrangement for increased sensitivity) mounted at the root to measure the blade tip deflection amplitude and frequency.

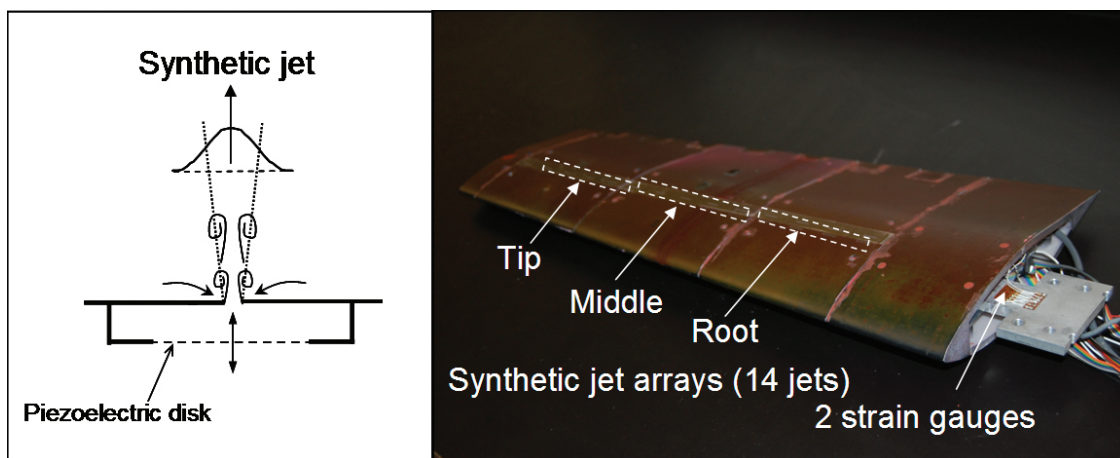


Figure 1. Experimental S809 wind turbine blade model and synthetic jet schematic.

2.2. Active flow control techniques

There are various types of actuators utilized to manipulate or control the flow field of wind turbine blades. We can classify most of them into two main categories: fluidic actuators and moving surface actuators. Moreover, both of these types of actuators can be applied near the leading edge or trailing edge of the airfoil, where their effect is markedly different as shown in **Figure 2**. Actuators mounted on the trailing edge of the blade manipulate the airfoil circulation, Γ thereby changing the lift per unit span, L' according to the Kutta-Joukowski theorem; $L' = \rho V \Gamma$. This can result in an increase or decrease in the lift coefficient compared to the baseline for a wide range of angle of attack, α , such that a change in lift coefficient, ΔC_L , bounds the baseline value as depicted in **Figure 2a**. On the other hand, actuators such as synthetic jets mounted near the airfoil leading edge are effective only for a small range of angles of attack; typically when the flow has separated in the vicinity of the synthetic jet. In these cases, active flow control is able to delay stall by partly reattaching the mean flow, thereby increasing the baseline stall angle of attack and maximum lift coefficient by ΔC_L , as shown in **Figure 2b**. More specifically, the separating shear layer shown schematically in **Figure 2c** at a certain shedding frequency is receptive to synthetic jet actuation at actuator input frequencies

at least an order of magnitude higher. The interaction between the synthetic jet and cross-flow creates a localized recirculation bubble that imparts momentum to the separating boundary layer causing the flow to reattach to the surface as shown schematically in **Figure 2d**.

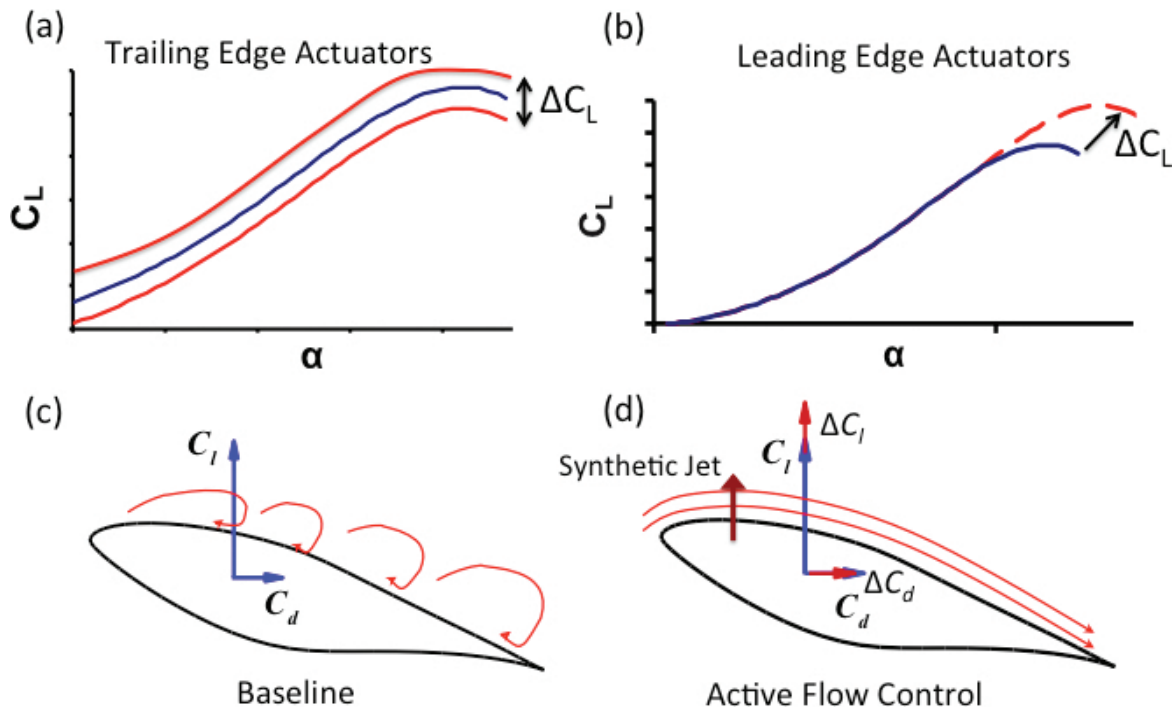


Figure 2. Active flow control modes on lift: (a) trailing edge actuators, (b) leading edge actuators, (c) baseline, and (d) active flow control.

When this occurs, there is a finite increase in lift coefficient and a decrease in drag coefficient, C_d (reduction in pressure or separation drag), which improves the aerodynamic efficiency of the blade as measured by the lift-to-drag ratio.

Plasma or dielectric barrier discharge actuators are characterized by very short response times and low power consumption. The main drawback is that they require very large AC voltage amplification and amplifiers in the range of 10–25 kV. In addition, they typically produce lower electric wind velocities compared to piezoelectric-based synthetic jets. Moving surface actuators include such devices as active microtabs, trailing edge flaps/gurney flaps, and vortex generators. Typically, they are driven by electromechanical means, whether it might be a servo motor or piezoelectric materials. The advantages of these actuators are that they have a considerable effect on the flow to change the aerodynamic properties (i.e., lift and drag) of an airfoil. However, they generally rely on more complex lower bandwidth mechanical actuation compared to fluidic actuators, and they may be considered as a lower research-oriented approach. Fluidic actuators include steady or unsteady blowing/suction devices and synthetic jet actuators. **Figure 3** displays schematics for three of the most common types of active flow control actuators: (i) plasma actuator, (ii) trailing edge flap, and (iii) piezo-based synthetic jet. We concentrate our discussion on the principle of operation for piezoelectric disk-based synthetic jets actuators.

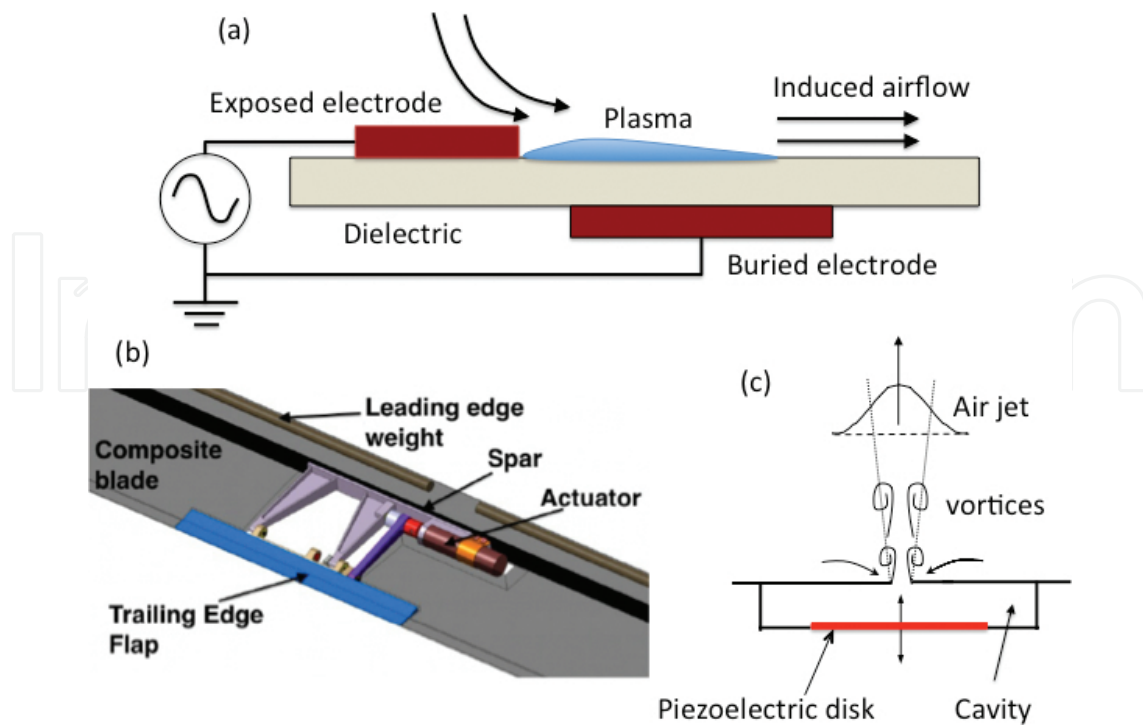


Figure 3. Active flow control actuator schematics: (a) plasma actuator, (b) trailing edge flap, and (c) piezoelectric synthetic jet actuator.

2.3. Piezoelectric synthetic jet actuator

The synthetic jet contains zero-net-mass flux and is synthesized by the time-harmonic formation and subsequent interactions of a train of vortex pairs that are formed at the edge of the orifice by the motion of a piezoelectric disk mounted in a sealed cavity. During the piezo upstroke, fluid is ejected from the cavity. The flow separates at the edge of the orifice forming a vortex sheet that rolls into a vortex pair and moves away from the orifice under its self-induced velocity [38]. During the piezo downstroke moving away from the orifice, the vortex pair has emanated sufficiently away from the orifice and is unaffected by the ambient fluid that is drawn into the cavity. The synthetic jet therefore imparts nonzero mass and impulse momentum for each vortex pair that is produced. The strongest vortex trains are produced when the piezo disk is driven at resonance with a certain optimum frequency determined via calibration with a hot-wire anemometer. The calibration process is depicted in the flowchart of **Figure 4**. An electronic signal generator is utilized to generate a sinusoidal signal of varying frequency. Depending on the piezo characteristics and cavity volume and geometry, the optimum driving frequency may be in the range of 1–2 kHz. The output channel of the signal generator is connected to the input channel of a piezo amplifier to amplify the voltage to a functional range for the piezoelectric disk. For most piezo disks, this voltage should not exceed 50 V in order to avoid damaging the piezo. The output of the piezo amplifier channel is then connected to the two piezo disk terminals while mounted to the cavity location on the wind turbine blade. Mounting the piezo disk is an important consideration; in order to create maximum momentum transfer, the piezo must be mounted semirigidly. In other words, the

piezo should be bonded with a flexible silicon-based sealant to allow maximum vertical deflection while also ensuring there is no air leaks around the perimeter of the piezo disk.

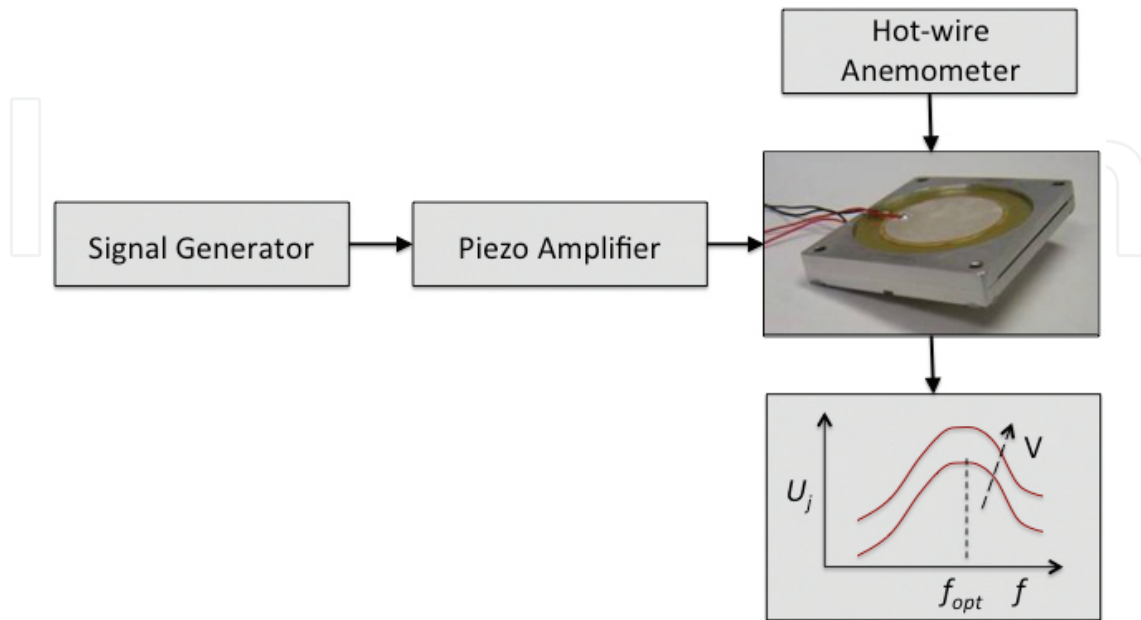


Figure 4. Synthetic jet actuator calibration process.

A hot-wire anemometer is utilized to measure the synthetic jet velocity, U_j , for a range of frequencies. The sensing element of the hot-wire probe is carefully placed in the middle of the orifice at the jet exit plane. The frequency of the sinusoidal signal is incrementally adjusted from a relatively low frequency with a step-size of about 50 Hz. As the frequency is increased, the velocity measured is observed to exhibit a somewhat linear relationship and gradually taper and reach a maximum at the optimum frequency, then decrease monotonically. This frequency is said to produce the maximum synthetic jet velocity, which is desired for most effective flow control performance. The calibration above should be repeated for several values of input piezo voltage. As **Figure 4** suggests, the synthetic jet velocity increases with higher voltage for a given frequency input. For modern piezo-based synthetic jet actuator techniques, jet velocities of 30 m/s and higher are possible.

The strength of a synthetic jet relative to the free-stream flow is quantified using the momentum coefficient, C_μ , defined as

$$C_\mu = \frac{nI_j}{\frac{1}{2}\rho U_\infty^2 A_w} \quad (1)$$

where U_∞ is the blade area, ρ is the air density, and n is the number of synthetic jets activated. I_j is the time-average jet momentum calculated only during the blowing portion of the actuation cycle, defined as

$$I_j = \frac{1}{\tau} \rho A_{sj} \int_0^\tau u_j^2(t) dt \quad (2)$$

where τ is the synthetic jet outstroke time (half the input frequency period), A_{sj} is the area of the synthetic jet orifice, and $u_j(t)$ is the centerline velocity at the jet exit plane. The time-average jet momentum is defined only for the outstroke part of the cycle. The centerline velocity is determined experimentally with a hot-wire anemometer.

2.4. Wind turbine blade techniques

Wind turbine blade models are typically tested inside a wind tunnel or outdoors where the atmospheric boundary layer (ABL) provides the inflow conditions. The advantage of a wind tunnel is that the inflow conditions can be controlled, whereas the ABL inflow conditions (such as velocity profile and turbulence intensity) cannot be changed; they are variable and must be measured prior to performing flow control on the blade. In this section, we focus on wind tunnel testing, which is the natural experimental tool of choice when investigating the fluid dynamics of novel flow control techniques or blade designs.

The wind tunnel experiments related to the wind turbine blade of **Figure 1** were conducted in an open-return low-speed wind tunnel. The test section has an 80 cm x 80 cm cross-section and is 5 m long. The wind tunnel is capable of achieving speeds up to 50 m/s and a turbulence level of less than 0.25%. The wind turbine blade model was mounted to one of the sidewalls of the test section on a pitch actuator capable of generating static blade pitch angles of attack, as well as unsteady angle of attack motions by prescribing a dynamic pitch waveform. The motion controller was implemented in xPC Target, a real-time operating system from Mathworks for control development. The blade pitch actuator is a DC-motor-based system with an optical encoder for position feedback, enabling angular position to 0.01° . The flow over the wind turbine blade must be quantified in terms of the Reynolds number, which is a non-dimensional parameter that relates the inertial forces of the blade relative to the viscous forces. The distinction must be made whether the flow is likely to be laminar, transitional, or turbulent. The actual flow depends on factors such as airfoil or blade surface finish, steadiness of the flow, and absence of disturbances. Generally speaking however, flat plate laminar flow can be expected for Reynolds numbers below 500,000, transitional flow in the range of 500,000 to one million, and fully turbulent flow for Reynolds numbers above one million. The Reynolds number based on blade chord is defined as

$$Re_c = \frac{U_\infty c'}{\nu} \quad (3)$$

where c' is the mean aerodynamic chord of the blade and ν is the air kinematic viscosity. For the blade model of **Figure 1** tested in the wind tunnel with experimental results presented in the next section, the Reynolds numbers were in the range of between 71,000 and 238,000. This flow can be considered as laminar flow.

The blade model was instrumented with a pair of strain gauges to measure blade structural vibration by quantifying its unsteady tip deflection. The strain gauges were surface mounted on the upper and lower surfaces of the blade's aluminum spar near the root. This created a Wheatstone half-bridge, where each gauge produced an equal but opposite magnitude strain, resulting in improved resolution of the strain reading. The strain gauges were oriented in the span-wise direction to capture the bending movements of the model (i.e., the deflections that are correlated to the roll moment). The voltage output from the strain gauges due to span-wise bending was correlated to the deflection at the tip. First, the voltage output was calibrated to the tip deflection by manually loading the blade with multiple equal weights (at the tip) and measuring its deflection. A second-order curve of the tip deflection as a function of voltage was then fitted to the data points and was integrated into the code to generate the time histories of the tip deflection.

2.4.1. Particle image velocimetry

PIV is an optical method of flow diagnostics utilized in experimental fluid dynamics research. It is utilized to obtain instantaneous velocity measurements and related turbulence properties in fluids. The fluid is seeded with small tracer particles designed to follow the flow and faithfully represent the flow dynamics. Together with a laser source to illuminate the particles and one or two charge-coupled device (CCD) cameras to take a pair of images of the particles in a fluid, the motion of the particles can be tracked to compute the velocity of the flow being studied.

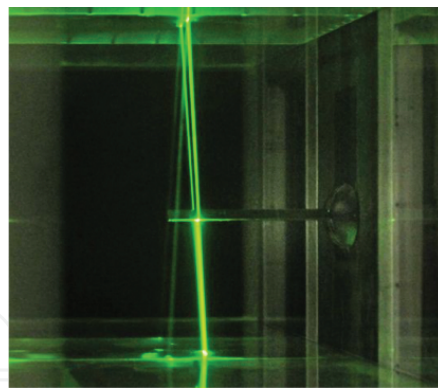


Figure 5. Measuring the flow with PIV on a wind turbine blade model.

The flow field over the suction surface of the blade was measured using PIV at a span-wise location of $y/b = 0.47$ (about mid span) coinciding with the middle of a synthetic jet orifice to capture maximum flow control effectiveness. The PIV system consists of a 1376 x 1040 pixel resolution thermoelectrically cooled 12-bit CCD camera, a pair of pulsed 120 mJ Nd:YAG lasers, and a programmable timing unit. In the present experiments, 2-D PIV data were acquired where a single CCD camera was mounted on a computer-controlled three-axis traverse. The laser light sheet was emitted from a free-moving optical arm and a laser head with variable lenses that can be positioned at any location along the outside of the test section.

With this arrangement, precise positioning of the laser light sheet was obtained. **Figure 5** is a photograph of the wind turbine blade tested during the PIV measurements; notice the vertical laser sheet, which emanates from top to bottom utilizing laser optics.

A smoke generator (model Magnum 800 made by Martin Manufacturing PLC) was used together with water-based fluid to provide droplets in the order of a few micrometers in diameter to serve as flow tracers. The smoke was introduced into the tunnel via the wind tunnel fan's air filter. The stream-wise and cross-stream velocity components (U , V) were computed from the cross-correlation of pairs of successive images with 50% overlap between the interrogation domains. For the time-averaged velocity vector fields, 250 image pairs were processed using an advanced multi-pass method where the initial and final correlation passes were 64×64 pixels and 32×32 pixels, respectively. The camera was mounted at a perpendicular distance of approximately 1 m to the laser light sheet, such that the distance between pixels is up to $125 \mu\text{m}$. The maximum velocity (30.48 m/s) corresponds to an average displacement of approximately 8 pixels with an error of ± 0.1 pixels, which corresponds to a maximum error of $\pm 1.25\%$ of the free-stream velocity (± 0.38 m/s at the maximum speed).

2.4.2. Load cell and surface pressure measurements

Active flow control for wind turbine blades is often applied as a technique to regulate the aerodynamic loads of the blade. These unsteady loads lead to blade structural vibration due to periodic flow separation on some portion of the blade. The most direct and accurate manner to measure blade loads (e.g., lift and drag) is to mount the blade on a multi-axis load cell or force transducer. The load cell is typically mounted onto a pitch actuator to change the blade angle of attack. The pitch actuator is then fixed to the sidewall of the wind tunnel test section. Force data are collected with a modern data acquisition (DAQ) hardware and software such as Labview from National Instruments. When selecting a load cell and taking force measurements, care must be taken to obtain sufficient resolution in the measurement by estimating the maximum lift and drag generated (using an analytical approach) and the expected changes in these forces due to active flow control which are small in comparison.

Surface pressure measurements are made to acquire the pressure distribution around the suction and pressure surfaces of the blade. This technique normally involves placing an array of pressure ports distributed along the chord on the surface of the blade at a certain span-wise location(s). The pressure ports are connected on the inside of the blade to small flexible tubes, which are routed to exit the blade and test section. The pressure difference between a given pressure tap and the reference free-stream pressure inside the wind tunnel is measured using a pressure scanner transducer with around 32 channels for good pressure distribution resolution and subsequent normal force coefficient calculation. The objective of this method is to calculate the pressure coefficient at each pressure tap location for each test free-stream velocity and angle of attack. The pressure distributions can then be utilized to compute the normal and tangential force coefficients with numerical integration schemes. The lift and drag coefficients of the blade are finally calculated via a trigonometric relation of these coefficients with the angle of attack. It must be stated that calculating the lift and drag coefficients with this technique is only valid and reasonably accurate for small to moderate angles of attack,

where the flow is still globally attached to the surface of the blade and the velocity is fairly steady in order to obtain a valid pressure tap measurement. Moreover, a more accurate method to calculate the drag coefficient would be to measure the velocity deficit and thus momentum loss at the wake of the blade (typically about one chord length behind the blade trailing edge) utilizing a pressure rake or traversing a pitot tube across the wake.

3. Experimental results

The experimental methods discussed above were utilized to analyze various aspects of the performance of wind turbine blades. In this section, we describe some of the main research findings, which have been published by the author in various journals and conference proceedings. Perhaps some of the earliest work on the feasibility of piezoelectric synthetic jets for active flow control of wind turbine blades was reported by Maldonado et al. (2011) [39, 40], with a subsequent paper focusing on the S809 airfoil [41], which is the basis for the results presented below.

3.1. Structural vibration control

A wind turbine blade exhibits various levels of structural vibration due to prime factors as incoming flow conditions (e.g., wind speed level, turbulence) and flow separation on different portions of the blade. Flow separation induces structural vibration of the blade at its structural resonance or natural frequency; the more severe the flow separation, the larger the amplitude of vibration will be. Active flow control was utilized as a technique to partially reattach the flow at post-stall angles of attack. The effect of the synthetic jets on the structural vibration is presented in **Figure 6a** at a Reynolds number of 1.85×10^5 and angle of attack of $\alpha = 16.5^\circ$. The time histories of the blade tip deflection with and without flow control are presented. For the

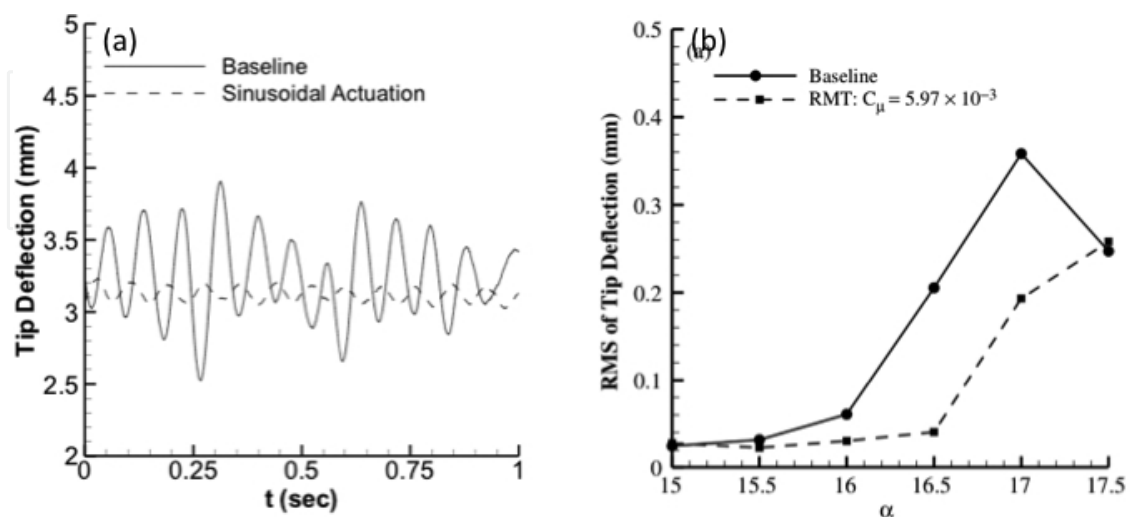


Figure 6. (a) Unsteady blade tip deflection and (b) RMS of blade tip deflection.

controlled case, the momentum coefficient of each synthetic jet is $C_{\mu} = 5.97 \times 10^{-3}$, where all 14 synthetic jets on the S809 blade of **Figure 1** were activated together. Without flow control, the blade vibrates at its fundamental structural resonance frequency, f_{struc} of around 6 Hz about its mean tip deflection of about 3.25 mm and average peak-to-peak amplitude of 0.8 mm. When the synthetic jets are activated, the peak-to-peak amplitude is reduced to about 0.13 mm; a reduction factor of 6 in the amplitude of vibration. The root mean square (RMS) of tip deflection as a function of the angle of attack is shown in **Figure 6a**. Flow control is effective in reducing vibration for a small range of post-stall angles of attack between 15° and 17.5° , where maximum vibration reduction occurs at 16.5° corresponding to the tip deflection time history of **Figure 6a**.

The effect of flow control on the structural vibration was also evaluated by computing the power spectral density (PSD) content as a function of frequencies present in the blade shown in **Figure 7a**. Without flow control, there is a noticeable peak at the structural frequency, f_{struc} of the blade. Using actuation, there is a reduction in all frequencies below 30 Hz. Furthermore, the magnitude of the structural peak decreases about an order of magnitude from the baseline level. This implies that the energy associated with the structural frequency vibration of the blade has greatly reduced. Another aspect of flow control is the ability to achieve proportional control of the blade tip deflection. This can be obtained by varying the momentum coefficient of the synthetic jets (i.e., their strength). **Figure 7b** presents the effect of the momentum coefficient on the PSD structural peak, where all the synthetic jets were activated. The figure clearly shows that proportional control of the tip deflection is achieved by simply varying the momentum coefficient.

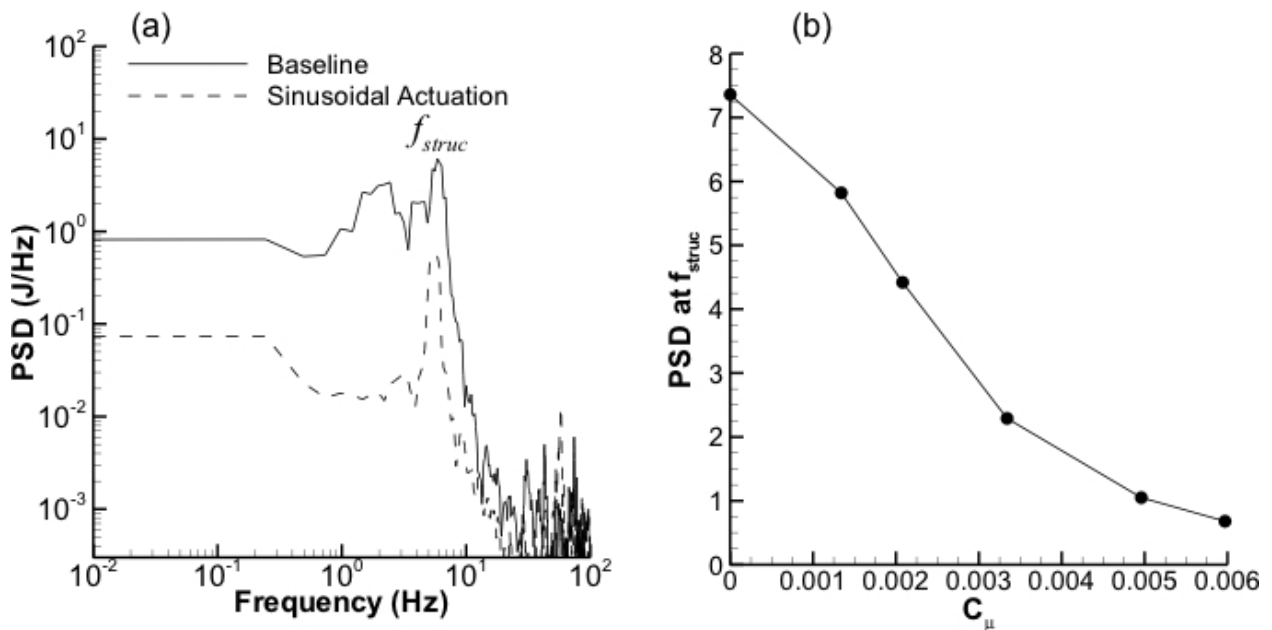


Figure 7. Power spectral density: (a) as a function of frequency and (b) power spectral density of structural vibration as a function of jet momentum coefficient.

3.2. PIV flow field measurements

Activation of the synthetic jets yields profound effects on the vibration of the blade due to flow reattachment. In order to quantify the ability for flow control to delay flow separation, 2-D PIV measurements of the mean global flow on the suction surface of the blade were conducted and are presented in **Figures 8** and **9** for the baseline and forced ($C_{\mu} = 5.97 \times 10^{-3}$) cases, respectively. The PIV plane was placed at $y/b = 0.47$, in the middle of a synthetic jet orifice for maximum control effectiveness. **Figures 8** and **9** present superimposed span-wise vorticity contours and streamlines for $\alpha = 15^\circ, 15.5^\circ, 16^\circ, 16.5^\circ, 17^\circ$, and 17.5° . Without flow control, the stream-wise

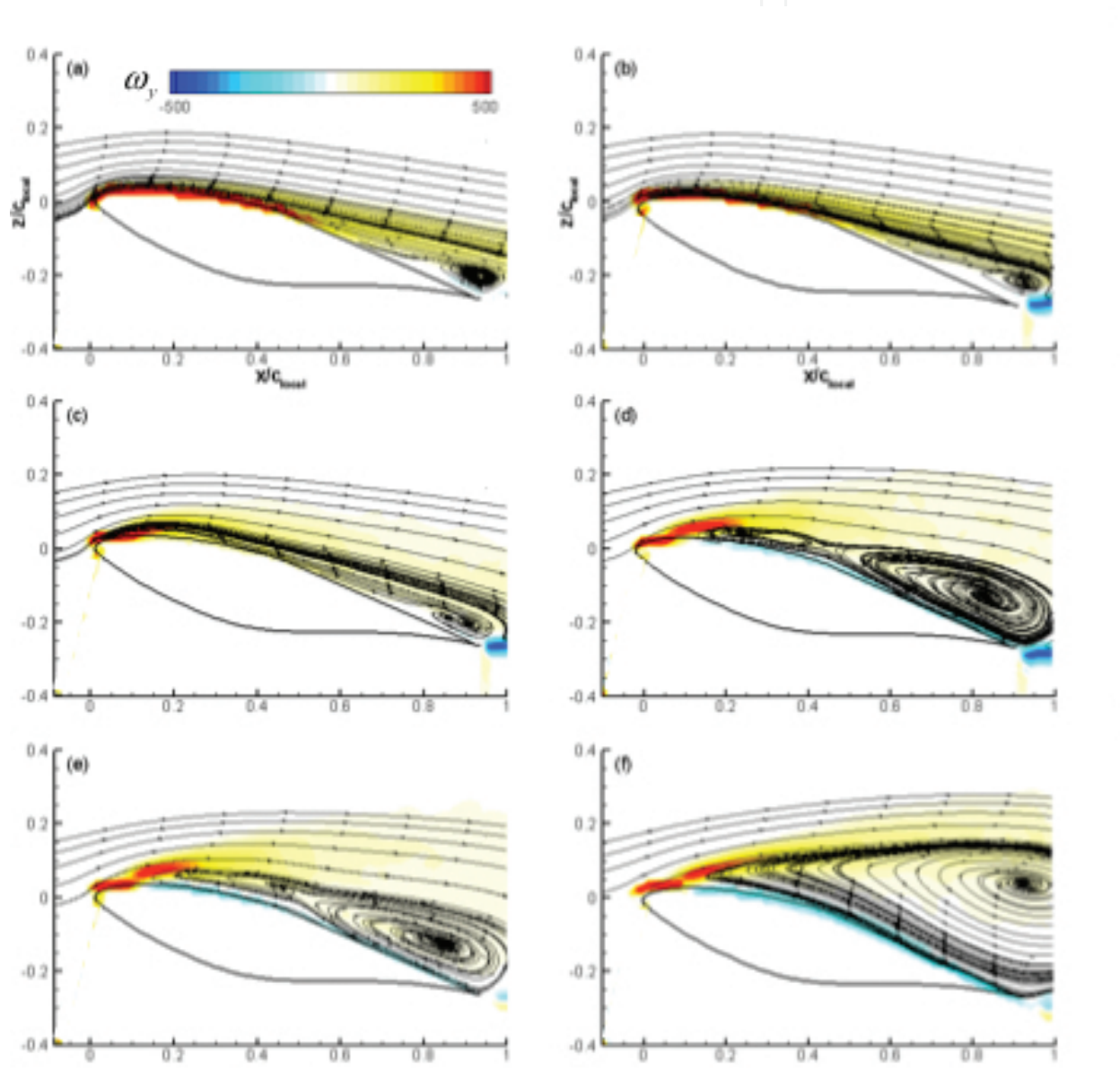


Figure 8. Superimposed span-wise vorticity and streamlines for the baseline case at $y/b = 0.47$ and $Re = 1.85 \times 10^5$. $\alpha = 15^\circ$ (a), 15.5° (b), 16° (c), 16.5° (d), 17° (e), and 17.5° (f).

and cross-stream extent of the separated flow increase as the angle of attack increases; this explains the increase of the RMS of tip deflection with angle of attack.

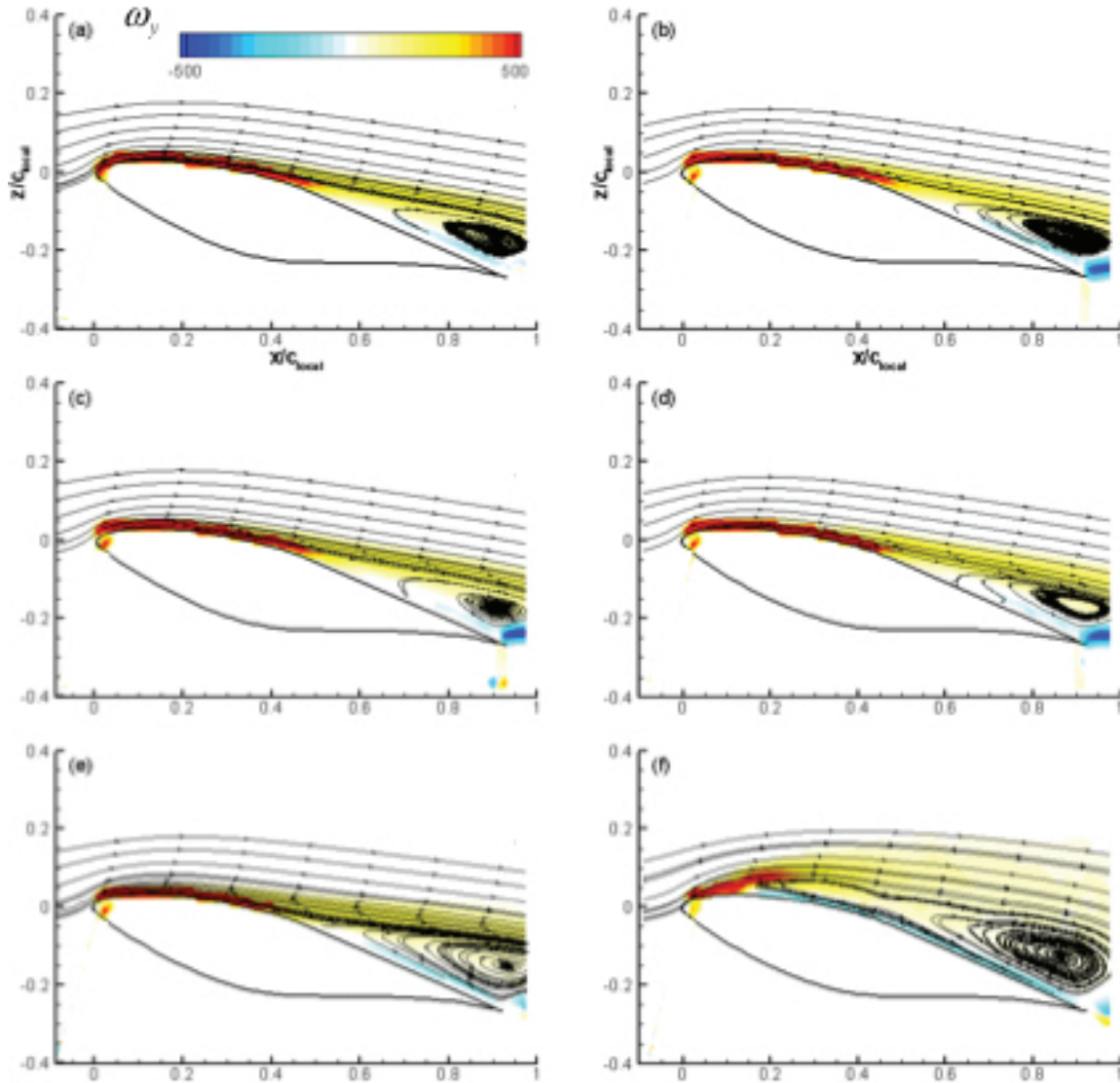


Figure 9. Superimposed span-wise vorticity and streamlines for the forced case at $y/b = 0.47$ and $Re = 1.85 \times 10^5$. $\alpha = 15^\circ$ (a), 15.5° (b), 16° (c), 16.5° (d), 17° (e), and 17.5° (f).

When flow control is applied (**Figure 9**), the flow field at $\alpha = 15^\circ$ and 15.5° (**Figure 9a** and **(b)**, respectively) is very similar to the baseline; thus, there is minimal effect on the tip vibrations at these angles of attack as seen in **Figure 6b**. However, as the angle of attack increases, the degree of flow separation is significantly reduced when flow control is applied (**Figure 9c-f**). These results qualitatively help explaining the trends in **Figure 6b**, where the RMS of tip deflection stays almost constant for the forced case up to $\alpha = 16.5^\circ$, while for the baseline case there is a sharp increase in RMS values. This is directly related to the extent and severity of the

flow separation and reattachment. At higher angles of attack (i.e., $\alpha = 17^\circ$ and 17.5° , **Figure 9e** and **(f)**, respectively), flow control is able to significantly reduce the flow separation. It is reasonable to conclude that the reduction in the extent of flow separation is predominantly responsible for reducing structural vibration of the blade.

4. Frontiers of active flow control research

The majority of the work in active flow control has been conducted with stationary and non-rotating wind turbine blades in order to simplify the interaction of the external cross-flow and the synthetic jet, leading to an understanding of the flow physics. In the process, the capabilities of flow control in the context of improving fluid dynamic and aerodynamic performance have been largely determined. The next logical step for investigators is to develop active flow control techniques for complex vortex-dominated flows, representative of actual rotating wind turbine blades and rotors. Some recent studies for rotating wind turbines include the use of a trailing edge flap [42] and other studies have been implemented on rotating blades for dynamic stall on helicopters [43, 44].

The author has recently embarked on establishing a research program for rotating wind turbine blades at the University of Texas at San Antonio. A rotor test tower facility was designed and constructed to investigate various wind turbine flow control topics of interest ranging from wake turbulence evolution and downstream impact, blade tip vortex breakdown, blade structural vibration/noise reduction, and energy capture efficiency. One of the fundamental concerns of wind farms is that wind turbines suffer from electric power loss due to the wake interaction of successive rows of wind turbines. The tip vortices generated from wind turbine blades are highly turbulent wake structures that may extend many rotor diameters downstream and reduce the power output and shortens the lifetime of the rotor of downstream turbines. For full-wake conditions, power losses of downstream turbines can be 30–40%, and when averaged over different wind directions, losses of 5–8% are reported [45]. The author's current project seeks to advance the understanding of vortex structure formation and breakdown on a small-scale wind turbine utilizing synthetic jets. Novel active flow techniques based on the methods presented earlier are used with an a priori understanding of the flow physics. Particle image velocimetry is utilized to experimentally measure coherent vortex structures and their turbulence characteristics to identify the most energetic scales that are susceptible to synthetic jet excitation and breakdown. The author theorizes that the larger scales can be "broken-down" into smaller turbulence scales with lower turbulent kinetic energy and strength, such that the adverse impact of the tip vortex on the inflow conditions and operation of a downstream turbine is mitigated. It is also believed that the amplitude of structural vibration of the blades is also diminished by the breakdown of large turbulent scales, which have a greater role in influencing blade resonance at its natural frequency.

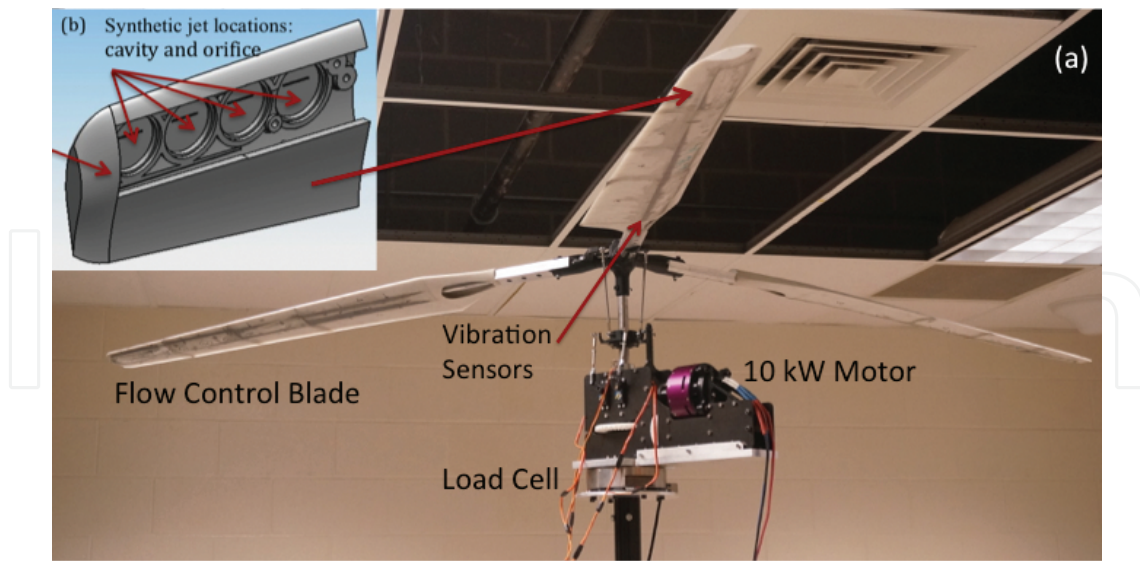


Figure 10. Rotor test tower facility for active flow control research.

The upper portion of the rotor test tower showing a rotor instrumented with synthetic jet slots is shown in **Figure 10a**. The rotor is powered by a 10-kW electric motor with a high-torque geared down transmission and collective/cyclic blade pitch capability mounted on a six-component load cell to measure rotor thrust and torque. A hall-effect sensor and magnet on the rotating shaft allow measurement of the rotor rotational velocity. The rotor shown contains a diameter of 2.41 m and the blades were custom designed in CAD with an S809 airfoil section and zero twist distribution. The blade has a span of 1.06 m and tapers down from a root chord of 0.178 m to a tip chord of 0.0889 m. A unique feature is the modular design of the blades; they are fabricated with additive manufacturing in sections to allow for modification to the blades, that is, changes to the geometry and/or location of the synthetic jet orifices. The tip section of the blade with four piezoelectric disk slots is shown in **Figure 9b**. The blade contains a total of 20 piezoelectric disk actuators and rectangular orifices placed at the quarter chord (0.25 c) of the airfoil as shown in the blade prototype of **Figure 11**.



Figure 11. S809 wind turbine blade prototype with synthetic jet actuators.

A 24-conductor slip ring is mounted to the rotor hub and transfers electrical signals between the synthetic jet actuators on the rotating blades and the stationary piezoelectric amplifier.

Finally, a high-power 10 kW supply powers the motor, and a National Instruments data acquisition system with Labview integrates the hardware for sensor measurements and actuator control.

Preliminary rotor thrust and torque measurements have been obtained in the Winter of 2015 for the baseline case without flow control at low rotor rotational velocities and blade pitch angles. The objective of these measurements was to validate operation of the tower and to observe tower vibration response for safe operation. Further experiments include the thrust, torque, and blade vibration measurements with and without flow control, as well as phase-locked stereoscopic (three velocity components) PIV flow measurements over the top suction surface of the blade and synthetic jets. The goal is to first characterize and understand the vortex flow nature of the rotor before attempting to perform flow control to influence and breakdown the turbulent vortex scales.

5. Conclusions

The wind energy industry is benefiting from the development of active flow control actuators and techniques to restore performance in wind turbines. As wind turbine rotor diameters continue to grow in order to reduce the cost of energy, the industry will require localized flow control along the blades to regulate unsteady blade loads and fatigue stress. This is critical in order to extend the life of the blades and other gearbox components. While some flow control technology such as trailing edge tabs have been demonstrated for aerodynamic load control in laboratories and large-scale field wind turbines, other flow control techniques and theories are still strictly being researched in the laboratory. This includes most notably the use of piezoelectric and plasma synthetic jet actuators for the control of vortex flow in rotating blades, blade tip vortex breakdown for vibration/noise reduction and to reduce wake turbulence levels for downstream wind turbines, and finally advanced closed-loop flow control techniques with blade sensors that adapt to the local flow conditions. Such concepts will be demonstrated in large-scale field turbines in the future, and wind energy will undoubtedly continue to be a growing source of renewable energy and an integral component of the US energy portfolio.

Author details

Victor Maldonado

Address all correspondence to: victor.maldonado@utsa.edu

Department of Mechanical Engineering, University of Texas at San Antonio, One UTSA Circle, San Antonio, Texas, USA

References

- [1] D.T. Yen, C.P. Van Dam, R.L. Smith, and S.D. Collins, "Active load control for wind turbine blades using MEM translational tabs," 39th AIAA/ASME, Salt Lake City, Utah, 2001.
- [2] D.T.Y. Nakafuji, C.P. van Dam, J. Michel, and P. Morrison, "Load control for wind turbines – a non-traditional microtab approach," 40th, AIAA/ASME, Indianapolis, Indiana, 2002.
- [3] J.P. Baker, K.J. Standish, and C.P. van Dam, "Two-dimensional wind tunnel and computational investigation of a microtab modified S809 airfoil," 43rd AIAA/ASME, Tucson, Arizona, 2005.
- [4] R. Chow, and C.P. van Dam, "Computational investigations of deploying load control microtabs on a wind turbine airfoil," 45th AIAA/ASME, Reno, Nevada, 2007.
- [5] S. Joncas, O. Bergsma, and A. Beukers, "Power regulation and optimization of offshore wind turbines through trailing edge flap control," 2005 ASME Wind Energy Symposium, Reno, Nevada, 2005.
- [6] N. Troldborg, "Computational study of the Riso-B1-18 airfoil with a hinged flap providing variable trailing edge geometry," *Wind Engineering*, 2005; 29: 89–113.
- [7] P.B. Andersen, M. Gaunaa, C. Bak, and T. Buhl, "Load alleviation on wind turbine blades using variable airfoil geometry," European Wind Energy Conference, Athens, 2006.
- [8] S. Basualdo, "Load alleviation on wind turbine blades using variable airfoil geometry," *Wind Engineering*, 2005; 29: 169–182.
- [9] C. Bak, M. Gaunaa, P.B. Andersen, T. Buhl, P. Hansen, K. Clemmensen, and R. Moeller, "Wind tunnel test on wind turbine airfoil with adaptive trailing edge geometry," 45th AIAA Aerospace Sciences Meeting and Exhibit, Reno, 2007.
- [10] M. Gaunaa, "Unsteady 2D potential-flow forces on a thin variable geometry airfoil undergoing arbitrary motion," Technical Report Risø-R-1478(EN), Risø, 2006.
- [11] T. Buhl, M. Gaunaa, C. Bak, "Potential of load reduction using airfoils with variable trailing edge geometry," *Journal of Solar Energy Engineering*, 2005; 127: 503–516.
- [12] C. Tongchitpakdee, S. Benjanirat, and L.N. Sankar, "Numerical studies of the effect of active and passive circulation enhancement concepts on wind turbine performance," *Journal of Solar Energy Engineering*, 2006; 128: 432–444.
- [13] T. Vronsky, "High performance cost-effective large wind turbine blades using air-jet vortex generators," ETSU W/41/00541/REP, 2000.

- [14] R.C. Nelson, T.C. Corke, H. Othman, M.P. Patel, S. Vasudevan, and T. Ng, "A smart wind turbine blade using distributed plasma actuators for improved performance," 46th AIAA Aerospace Sciences Meeting, Reno, 2008.
- [15] M.L. Post and T.C. Corke, "Separation control using plasma actuators: dynamic stall vortex control on oscillating airfoil," *AIAA Journal*, 2006; 44: 3125–3135.
- [16] C.M. Ho and P. Huerre, "Perturbed free shear layers," *Annual Review of Fluid Mechanics*, 1984; 16: 365–424.
- [17] D. Oster and I.J. Wygnanski, "The forced mixing layer between parallel streams," *Journal of Fluid Mechanics*, 1982; 123: 91–130.
- [18] F.A. Roberts. "Effects of periodic disturbances on structure of mixing in turbulent shear layers and wakes," PhD Thesis, California Institute of Technology, Pasadena, California, 1985.
- [19] A. Seifert, T. Bachar, D. Koss, M. Shepshelovich, and I. Wygnanski, "Oscillatory blowing: a tool to delay boundary-layer separation," *AIAA Journal*, 1993; 31: 2052–2060.
- [20] K.H. Ahuja and R.H. Burrin, "Control of flow separation by sound," AIAA-84-2298. AIAA/NASA 9th Aeroacoustics Conference, Williamsburg, VA, 1984; 15p.
- [21] D. Neuberger and I. Wygnanski, "The use of a vibrating ribbon to delay separation on two dimensional airfoils. Proceedings of Air Force Academy Workshop in Unsteady Separated Flow, Colorado Springs, CO, 1987.
- [22] I. Wygnanski, "Some observations affecting the control of separation by periodic excitation," *AIAA Paper* 2000-2314, 2000.
- [23] M. Amitay and A. Glezer, "Role of actuation frequency in controlled flow reattachment over a stalled airfoil," *AIAA Journal*, 2002; 40: 209–216.
- [24] M. Amitay, M. Horvath, M. Michaux, and A. Glezer, "Virtual aerodynamic shape modification at low angles of attack using synthetic jet actuators," *AIAA Paper* 2001-2975, 2001.
- [25] Amitay M, Glezer A. Controlled transients of flow reattachment over stalled airfoils. *International Journal of Heat and Fluid Flow*, 2002; 23: 690–699.
- [26] M. Amitay and A. Glezer, "Flow transients induced on a 2-D airfoil by pulse-modulation actuation," *Experiments in Fluids*, 2006; 40: 329–331.
- [27] M. Amitay, D.R. Smith, V. Kibens, D.E. Parekh, and A. Glezer, "Modification of the aerodynamics characteristics of an unconventional airfoil using synthetic jet actuators," *AIAA Journal*, 2001; 39: 361–370.
- [28] T.R. Bewley, "Flow control: new challenges for a new Renaissance," *Progress in Aerospace Sciences*, 2001; 37: 21–58.

- [29] K. Cohen, S. Siegel, and T. McLaughlin, "Control issues in reduced-order feedback flow control," *AIAA Paper* 2004-0575, 2004.
- [30] C.W. Rowley, D.R. Williams, T. Colonius, R.M. Murray, D.G. MacMartin, and D. Fabris, "Model-based control of cavity oscillations," Part II. *AIAA Paper* 2002-0972, 2002.
- [31] L.N. Cattafesta, S. Garg, and M. Choudhari, "Active control of flow-induced cavity response," *AIAA Paper* 1997-1804, 1997.
- [32] L.N. Cattafesta, S. Garg, M.A. Kegerise, and G.S. Jones, "Experiments on compressible flow-induced cavity oscillations," *AIAA Paper* 1998-2912, 1998.
- [33] G. Berkooz, P. Holmes, and J.L. Lumley, "The proper orthogonal decomposition in the analysis of turbulent flows," *Annual Review of Fluid Mechanics*, 1993; 25: 539–575.
- [34] R.B. Cal and M. Gibson, "Proper orthogonal decomposition of a wind turbine array boundary layer," 6th AIAA Theoretical Fluid Mechanics Conference, Honolulu, HI, 2011.
- [35] M. Melius, R.B. Cal, and K. Mulleners, "Dynamic stall of an experimental wind turbine blade," *Physics of Fluids*, 2016; 28: 034103.
- [36] D.S. Berry, "Blade system design studies phase 2: final project report," Sandia Report, SAND2008-4648, 2008.
- [37] D.M. Somers, "Design and experimental results for the S809 airfoil," NREL/SR-440-6918, 1997
- [38] A. Glezer and M. Amitay, "Synthetic jets," *Annual Review of Fluid Mechanics*, 2002; 34: 503–529.
- [39] V. Maldonado, J. Farnsworth, W. Gressick, and A. Amitay, "Active control of flow separation and structural vibrations of wind turbine blades," *Wind Energy*, 2010; 13: 221–237.
- [40] V. Maldonado, J. Farnsworth, W. Gressick, and M. Amitay, "active enhancement of wind turbine blades performance", 27th AIAA/ASME Wind Energy Symposium, 2008, Reno, NV.
- [41] Maldonado, V., Boucher, M., Ostman, R., and Amitay, M., "Active vibration control of a wind turbine blade using synthetic jets," *International Journal of Flow Control*, 2010; 1: 4.
- [42] M.J. Balas and N. Li, "Adaptive flow control of rotating wind turbine blades based on the Beddoes-Leishman model using trailing-edge flaps", AIAA Guidance, Navigation, and Control Conference, AIAA SciTech (AIAA 2016-0624), San Diego, California.
- [43] H. Mai, G. Dietz, W. Geissler, K. Richter, J. Bosbach, H. Richard, and K. De Groot, "Dynamic stall control by leading-edge vortex generators," *Journal of the American Helicopter Society*, 2008 January; 53(1), pp. 26-36.

- [44] P. Martin, J. Wilson, J. Berry, T.C. Wong, M. Moulton, and M. McVeigh, "Passive control of dynamics stall," 26th AIAA Applied Aerodynamics Conference, Honolulu, Hawaii, 2008.
- [45] R.J. Barthelmie, S.T. Frandsen, N.M. Nielsen, S.C. Pryor, P.E. Rethore, and H.E. Jørgensen, "Modelling and measurements of power losses and turbulence intensity in wind turbine wakes at Middelgrunden offshore wind farm," *Wind Energy*, Vol. 10(6), pp. 517-528, 2007.

IntechOpen

IntechOpen